Journal of Alloys and Compounds, 177 (1991) 107–118
JAL 0073

Microstructural correlations with the hydrogenation kinetics of $FeTi_{1+x}$ alloys

S.-M. Lee and T.-P. Perng
Department of Materials Science and Engineering, National Tsing Hua University, Hsinchu (Taiwan)

(Received May 27, 1991)

Abstract

The influence of β-Ti on the hydrogenation properties of $FeTi_{1+x}$ alloys ($0.1 \leqslant x \leqslant 0.5$) was investigated. The surface morphologies and chemical compositions before and after hydrogenation were examined. From the cracking features of the surfaces and X-ray diffraction analysis, it was concluded that the hydride of β-Ti was formed prior to hydrogenation of the FeTi matrix in these alloys. Formation of TiH_2 induced cracking into the FeTi matrix. Hydrogen was then transported through the cracks and absorbed by FeTi. Therefore, activation treatment was not required. In addition, the rate of hydrogen absorption of these alloys in the first few cycles was faster than that of $FeTi_{1.0}$. The difference in the kinetics of the first hydrogenation cycle of these alloys can be explained on the basis of the amount and distribution of the eutectic strips.

1. Introduction

Hydrogen can be used as an ideal fuel for its high efficiency and non-pollution or as a substance for many types of energy conversion. In most cases, hydrogen is stored as a compressed gas or cryogenic liquid. However, the safety and cost of this storage are often the main concerns for its practical uses. Therefore, hydrogen stored as a metal hydride has become more promising recently because of its unique features.

Iron and titanium form two known stable intermetallic compounds, FeTi and Fe_2Ti [1]. Fe_2Ti does not absorb hydrogen, whereas FeTi was reported by Reilly and Wiswall [2] to react readily with hydrogen to form two hydrides, FeTiH and $FeTiH_2$. These hydrides may easily decompose and are useful as hydrogen storage media. However, the virgin compound of FeTi reacts very slowly with hydrogen at room temperature even at high hydrogen pressures. A high-temperature heat treatment is required in order to activate the sample to absorb hydrogen at room temperature.

Although the mechanism of activation has been investigated extensively [3–10], it is still not completely understood. It is generally acknowledged that the activation of FeTi is composed of two steps. The first step is a heat treatment which removes the surface oxide film, and the second step involves the hydrogen absorption–desorption cycling which generates new clean surfaces by cracking of the compound. Lee *et al.* [11–13] have studied the

0925-8388/91/$3.50

hydriding kinetics of activated FeTi. They reported that the initial rate of hydrogen absorption was controlled by chemisorption of the hydrogen molecules on the FeTi surface and the rate of later stage was controlled by hydrogen diffusion in the hydride layer.

The reversible transfer capacity of hydrogen in FeTi is decreased significantly with the hydrogenation and dehydrogenation cycles in the presence of other gases in hydrogen [14]. However, when a small amount of manganese is substituted for iron, the activation is promoted, the resistance to impure gases is enhanced, and the hydrogen storage capacity can be maintained [14]. In addition, it has also been reported that modified FeTi containing an additional ternary element does not need any special treatment prior to hydrogenation [15]. Although the influence of partial substitution of iron in FeTi by some other 3d transition metals has been widely investigated for some years, the cause for the effect is still not well understood.

Mizuno and Morozumi [16] have found that hydrogenation of titanium-rich alloys $FeTi_{1+x}$ $(0<x<1)$ occurs without any activation treatment and the surface sensitivity to poisoning by impurity gases can be reduced. Matsumoto *et al.* [17] have also reported that excess titanium enhances the activation of FeTi and that the formation of β-Ti hydride occurs prior to hydrogenation of the FeTi phase in the alloys. Owing to the large volume expansion of β-Ti during hydrogenation, a large number of cracks are created in the alloys and a highly reactive FeTi surface is obtained.

In this study, the hydrogenation of several $FeTi_{1+x}$ alloys containing β-Ti is investigated in more detail. The hydrogen absorption curves were compared. The microstructures, especially the morphologies of the specimen surfaces before and after hydrogenation, were carefully examined. The difference in the hydrogen absorption kinetics for these alloys was correlated with their compositions and microstructures.

2. Experimental details

Pure powders of iron (purity, 99.9 wt%) and titanium (purity, 99.5 wt%) were used as the starting materials. Compounds of $FeTi_{1+x}$ with $x=0$, 0.1, 0.2, 0.3, 0.4 and 0.5 were prepared in an arc furnace under an argon atmosphere. The ingots were turned and remelted five times during the arc-melting in order to homogenize the samples. No further annealing or homogenization of these alloys was conducted. All the alloys were quite brittle and could be easily pulverized into granules. They were crushed in an ambient atmosphere and only powders of $+20$ to -50 mesh were selected for the hydrogenation experiments. Before the experiment, the compounds were analyzed by powder X-ray diffraction (XRD).

The hydrogen absorption–desorption behavior was investigated using a high-pressure volumetric system [18]. For each run, approximately 7 g of powder was placed in the reactor vessel. One end of the reactor was provided with a thermocouple connector. The other end was connected by a 6.35

mm stainless steel tube to a high-pressure valve, which was then connected to the high-pressure manifold. The manifold had several 6.35 mm stainless steel tubes connecting to a pressure transducer, two vacuum gauges, and three high-pressure gas reservoirs. For reactions at $T < 80$ °C, a water bath was used to maintain the temperature with an accuracy of 0.2 °C. For the activation treatment, the reactor was heated with a small electric furnace.

Of the alloys studied here, only $FeTi_{1.0}$ needed to be activated. To activate $FeTi_{1.0}$, the reactor was first loaded with the sample, evacuated for about 30 min at room temperature and then 0.5 MPa of hydrogen gas (at least 99.99% pure) was admitted to the reactor. The reactor was heated to 400 °C for about 30 min and then cooled to room temperature. There was usually a slight drop in hydrogen pressure due to some absorption of hydrogen by the sample. After the activation, kinetics study of the alloy was started. The reactor was evacuated for about 30 min before introducing 4.0 MPa of hydrogen for the absorption experiment. The pressure change of hydrogen was recorded as a function of time.

The other samples did not need activation and were directly exposed to hydrogen at 4.0 MPa after the reactor had been evacuated for about 30 min. The hydrogen absorption curves (pressure *vs.* time) were obtained at 30 °C.

The microstructures of the powder samples before and after hydrogenation were examined by optical metallography and scanning electron microscopy (SEM). The compositions in the areas of interest were obtained by energy dispersive X-ray (EDX) analysis. The phases in the samples before and after hydrogenation were analyzed by XRD.

3. Results

The optical micrographs of five alloys of $FeTi_{1+x}$ are shown in Fig. 1. XRD analysis showed that both FeTi and β-Ti were present in these alloys. From the EDX analysis the matrix was identified to be the FeTi phase, whereas the strip regions were the eutectic mixture of FeTi and β-Ti. As the ratio of Ti/Fe increased, the content and width of the eutectic increased, whereas the size of the enclosed FeTi decreased.

For these alloys, hydrogen was readily absorbed without activation. Figure 2 shows the absorption rates for the unactivated alloys at 30 °C under an initial hydrogen pressure of 4.0 MPa. The hydrogen absorbed in each alloy [H] is normalized with respect to its saturated hydrogen content [H_s]. After a period of incubation, the hydrogen absorption rate gradually rises and then increases rapidly. The rate slows down again before approaching the saturated hydrogen content.

After one cycle of hydrogenation and dehydrogenation, the hydrogen absorption rates for these alloys became very rapid (saturation of hydrogen was completed in 200 s). For example, the hydrogen absorption curve for the second cycle of $FeTi_{1.2}$ at 30 °C is shown in Fig. 3(a). In contrast to

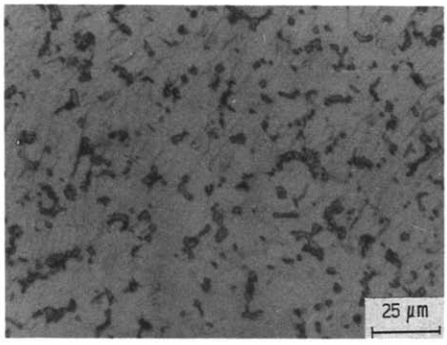

(a)

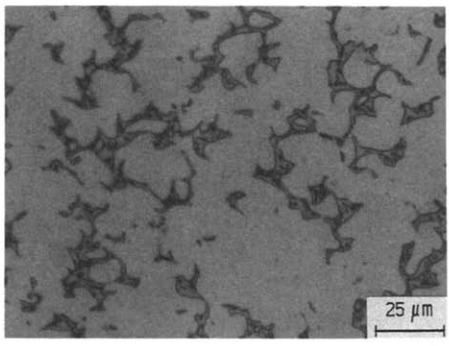

(b)

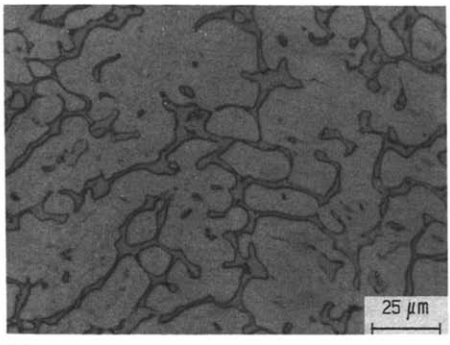

(c)

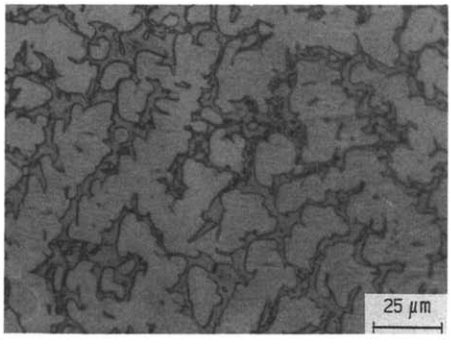

(d)

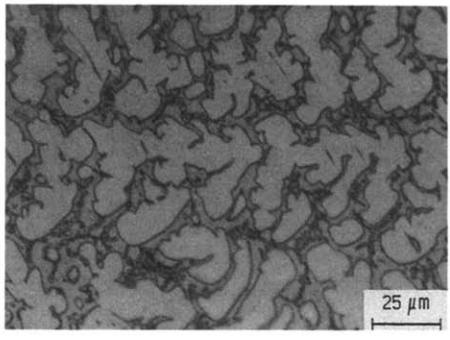

(e)

Fig. 1. Optical micrographs of the $FeTi_{1+x}$ alloys. (a) $FeTi_{1.1}$, (b) $FeTi_{1.2}$, (c) $FeTi_{1.3}$, (d) $FeTi_{1.4}$, and (e) $FeTi_{1.5}$.

the $FeTi_{1+x}$ alloys, the alloy with Fe/Ti = 1.0 needed repeated activation treatment several times before hydrogen absorption was initiated. Even after the alloy had been activated, the hydrogen absorption rates in the first few cycles remained slow and saturation of the alloy with hydrogen was never completed. Figure 3(b) shows eight successive hydrogen absorption curves of $FeTi_{1.0}$ after the activation treatment. All these hydrogenation cycles were

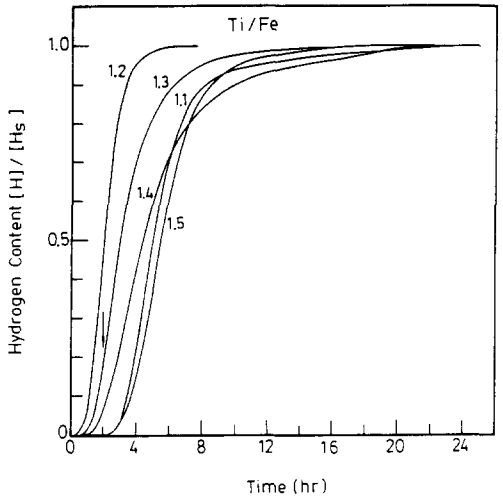

Fig. 2. Initial hydrogen absorption curves of the unactivated $FeTi_{1+x}$ alloys at 30 °C and 4 MPa of H_2.

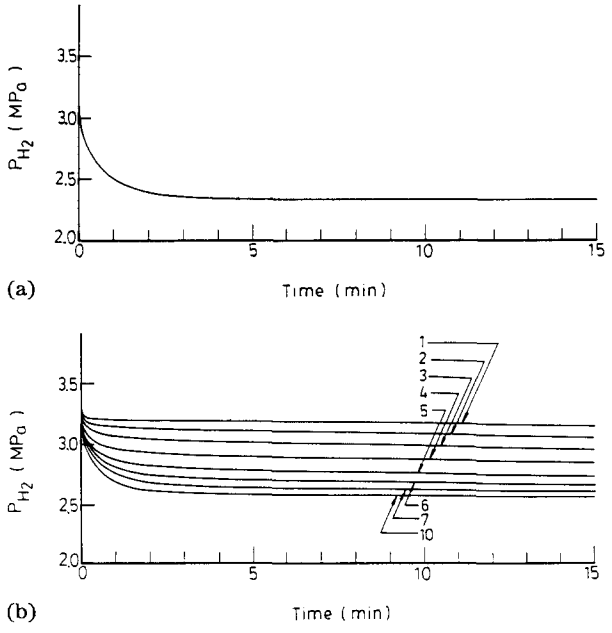

Fig. 3. (a) Hydrogen absorption curve for the second cycle of $FeTi_{1.2}$ at 30 °C. (b) Hydrogen absorption curves for various cycles of activated $FeTi_{1.0}$ at 30 °C.

started with 3.3 MPa of H_2. Saturation of hydrogen in $FeTi_{1.0}$ was reached only after it had been charged and discharged for about ten cycles. The rates of hydrogenation after the tenth cycle became faster and comparable with that of the second cycle of $FeTi_{1.2}$.

The surface morphologies of the hydrogenated alloys at various stages were examined by SEM. For example, Fig. 4(a) shows the micrograph of $FeTi_{1.3}$ after it has been exposed to hydrogen for 2 h, corresponding to the point indicated by an arrow on the curve of $FeTi_{1.3}$ in Fig. 2. Some cracks were already present. As the hydrogenation continued, an increasing number of cracks were induced. Figure 4(b) shows a micrograph of the same alloy after the hydrogenation has been completed. Many more cracks were observed. Within the large primary cracks around the edge of the micrograph, there are medium-sized cracks branching from them. Within these medium-sized cracks, there are still even smaller branched cracks. The chemistries of the regions around the cracks were analyzed by EDX. It was found that the regions around the large and medium-sized cracks were titanium-rich, whereas those around the smaller cracks had higher ratio of Fe/Ti, as compared in Fig. 5. The crack morphology can be compared with the optical micrograph of the virgin alloy (Fig. 1(c)) or more precisely with the SEM micrograph of the etched surface before hydrogenation (Fig. 4(c)). It is seen that the large and medium-sized cracks follow the paths of the eutectic strips. The size and shape of the area enclosed in these cracks are about the same as those of the FeTi phase. The XRD patterns of the alloy taken before and

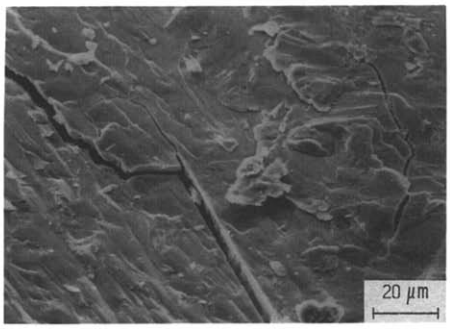

(a)

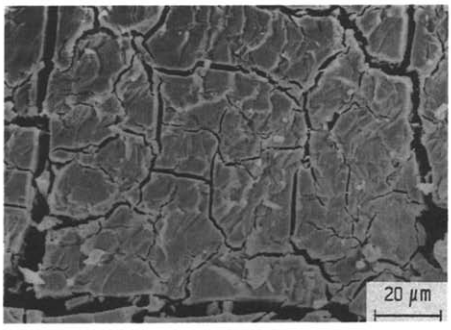

(b)

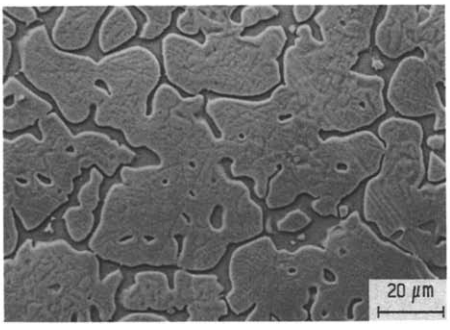

(c)

Fig. 4. SEM micrographs of $FeTi_{1.3}$: (a) exposed to hydrogen for 2 h; (b) after one cycle of hydrogenation; (c) etched surface before hydrogenation.

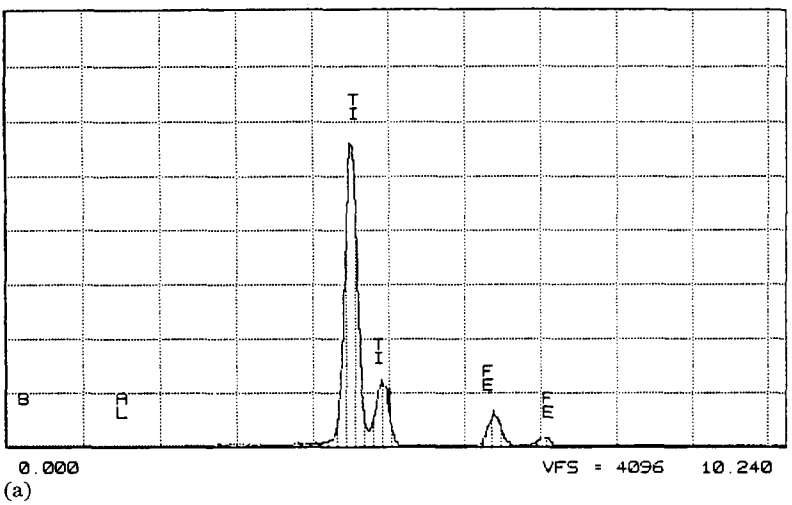

(a)

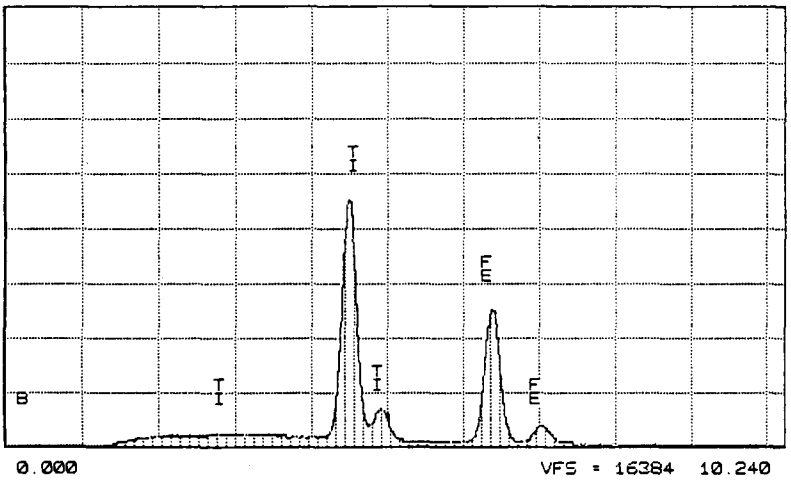

(b)

Fig. 5. EDX spectra of the areas around (a) the primary cracks and (b) the smaller cracks for $FeTi_{1.3}$.

after hydrogenation (Fig. 6) reveal that the β-Ti peaks have disappeared but some new diffraction lines corresponding to the titanium hydride are present after the cycling. All these observations imply that the large and medium-sized cracks are formed due to the hydrogenation of β-Ti, whereas the smaller cracks are generated due to the formation of $FeTiH_x$.

When the $FeTi_{1+x}$ alloys have been subjected to an increase in the number of hydrogenation cycles, the surface features remain essentially unchanged. The surface morphologies for $FeTi_{1.3}$ and other alloys after 20 cycles of hydrogenation are shown in Figs. 7(a)–(d). When the morphology in Fig. 7(b) is compared with that in Fig. 4(b), similar cracking features are observed for $FeTi_{1.3}$. The SEM micrographs for the $FeTi_{1+x}$ alloys can be compared with each other and with the optical micrographs of the corre-

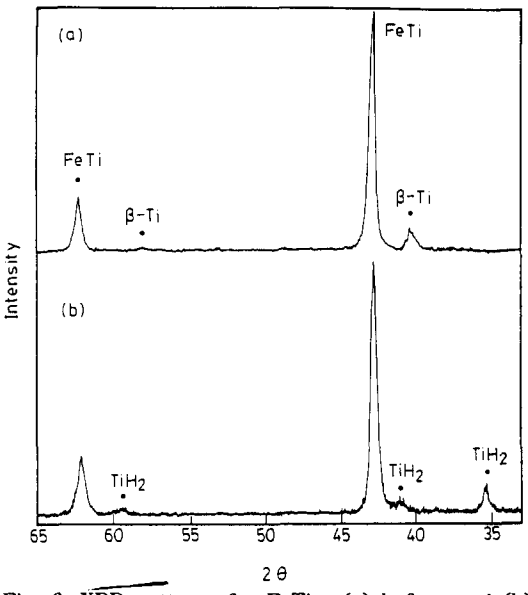

Fig. 6. XRD patterns for $FeTi_{1.3}$ (a) before and (b) after hydrogenation at 30 °C.

sponding virgin alloys (Fig. 1). Again, the paths of the larger cracks follow the eutectic strips. However, it is noted that the average size of these cracks decreases as x increases. The reason for this will be discussed in the next section.

4. Discussion

From the Fe–Ti binary phase diagram [1], the FeTi phase is homogeneous in the composition region $0.99 \leqslant Ti/Fe \leqslant 1.08$ (atomic ratio) at room temperature. If the composition is slightly deficient in titanium (*i.e.* $Ti/Fe < 0.99$), Fe_2Ti will form. The presence of Fe_2Ti is undesirable because it does not absorb hydrogen and is useless for hydrogen storage purposes [2]. However, if the composition is slightly enriched with titanium ($Ti/Fe > 1.08$), α- or β-Ti will precipitate.

Matsumoto *et al.* [17] have investigated the hydrogenation properties of alloys containing FeTi and β-Ti by using the *in situ* X-ray diffraction technique. From the change in the X-ray spectra, they proposed that the hydrogenation of β-Ti had occurred prior to hydrogenation of FeTi in the alloys. From Fig. 6, the titanium hydride could be indexed according to an f.c.c. lattice with $a \approx 0.443$ nm, whereas β-Ti was indexed according to a b.c.c. lattice with $a \approx 0.323$ nm [17]. The change in volume of β-Ti after hydrogenation was about 30%. Therefore, it is evident that the formation of titanium hydride would create a large number of cracks in the alloys. Since titanium hydride is more stable than $FeTiH_x$, it is formed prior to the

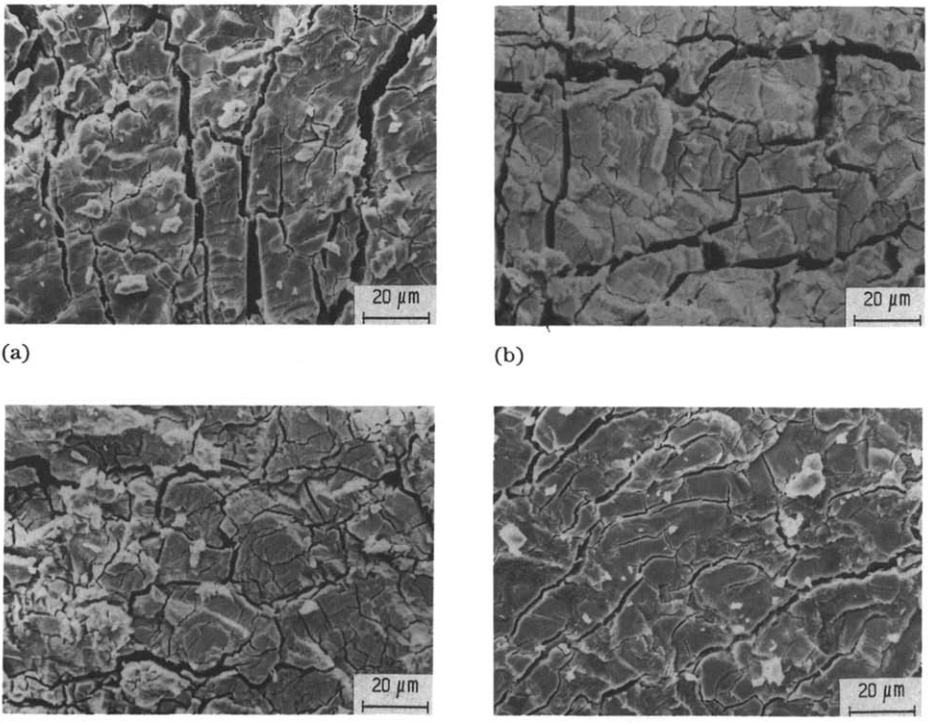

Fig. 7. SEM micrographs of the alloys after 20 cycles of hydrogenation. (a) $FeTi_{1.2}$, (b) $FeTi_{1.3}$, (c) $FeTi_{1.4}$, and (d) $FeTi_{1.5}$.

hydrogenation of the FeTi phase and persists in air for a long period of time.

The cracking features, EDX and XRD analyses, along with the *in situ* X-ray diffraction observation by Matsumoto *et al.* [17], suggest that the hydrogenation of $FeTi_{1+x}$ alloys occurs in the following sequence:

(1) In the initial stage of hydrogenation, the formation of titanium hydride, TiH_2, occurred first. The hydride was dispersed on the surface and might also penetrate into the particle.

(2) The large volume expansion of β-Ti during hydrogenation caused cracking along the eutectic strips and also induced smaller cracks in FeTi. New fresh surface of FeTi was continuously created during the hydrogenation of β-Ti.

(3) Hydrogen was absorbed by the new fresh surfaces of FeTi. The titanium hydride provided preferred path for fast hydrogen penetration into FeTi. Hydrogen entered FeTi by diffusion through the interior interface between the titanium hydride and FeTi.

The sequence of this process enables the $FeTi_{1+x}$ alloys to absorb hydrogen without activation. With this process in mind, it is now appropriate to examine the difference in the initial hydrogen absorption kinetics for the

$FeTi_{1+x}$ alloys. In Fig. 2, the initial hydrogen absorption rate of unactivated $FeTi_{1.1}$ is slower than those of $FeTi_{1.2}$ and $FeTi_{1.3}$. This can be explained by the micrographs of the $FeTi_{1+x}$ alloys in Fig. 1. The amount of β-Ti in $FeTi_{1.1}$ is less than that in $FeTi_{1.2}$. Therefore, the β-Ti dispersed on the surface layer generates fewer cracks in $FeTi_{1.1}$ than in $FeTi_{1.2}$. This leads to a slower hydrogenation rate for $FeTi_{1.1}$. However, when the amount of β-Ti further increases, the rate of hydrogen absorption is found to slow down. Too much β-Ti present in the $FeTi_{1+x}$ alloys becomes deleterious for the hydrogenation in the first cycle. This peculiar behavior is examined and explained as follows.

From the optical micrographs of Fig. 1, the eutectic strips consist of β-Ti and FeTi phases. The FeTi phase is present as small islands in the matrix of β-Ti. The fraction of the eutectic in the $FeTi_{1+x}$ alloys increases with x. In $FeTi_{1.2}$, the three-dimensional networks of eutectic are rarely seen except in some localized regions. Whereas in $FeTi_{1.3}$, $FeTi_{1.4}$ and $FeTi_{1.5}$, increasing numbers of three-dimensional networks are formed. The eutectic strips also become successively broader.

When these alloys are exposed to hydrogen, the hydrogen is preferentially absorbed by the β-Ti phase at first, owing to its higher stability. Formation of TiH_2 causes volume expansion and induces cracks along the eutectic strips. When the amount of β-Ti is small, the cracks will soon reach to the eutectic boundary. Since FeTi is very brittle, crack arrest by FeTi does not occur and further cracking into the FeTi phase is expected. However, when the amount of β-Ti is high, the cracks will propagate predominantly within the eutectic. As β-Ti is more ductile, the propagation of these cracks is slower and more difficult. There is less cracking into the FeTi phase.

The cracking process and hydrogenation kinetics of these alloys in the initial stage can be explained schematically by Fig. 8. The cross-section microstructures of $FeTi_{1.2}$ and $FeTi_{1.5}$ before hydrogenation are compared in Fig. 8(a). When they are exposed to hydrogen, some cracks begin to form in the eutectic (Fig. 8(b)). Since the eutectic strips are short and discontinuous in $FeTi_{1.2}$, the cracks soon propagate into the FeTi matrix and hydrogen may be transported through the crack and absorbed by the fresh surfaces. However, for $FeTi_{1.5}$ cracking through β-Ti is more difficult and more restricted. As there are more eutectic strips in this alloy, the volume change is greater and therefore more cracks are formed simultaneously. The crack width becomes smaller on average. The greater strain in the matrix also induces a higher compressive stress at the crack tips. Therefore, the cracking rate is lower than that in $FeTi_{1.2}$ (Fig. 8(c)). As hydrogenation continues, for $FeTi_{1.2}$, increasing cracks are induced in the FeTi matrix and therefore more hydrogen is absorbed by this phase. Whereas for $FeTi_{1.5}$, within the same period of time, cracking is primarily restricted within the eutectic (Fig. 8(d)).

As illustrated by this model, the average size of the primary cracks will decrease as the amount of eutectic increases. The sizes of the primary cracks in various alloys can be compared and distinguished by Fig. 7. As the surface after 20 cycles of hydrogenation is essentially the same as that after the

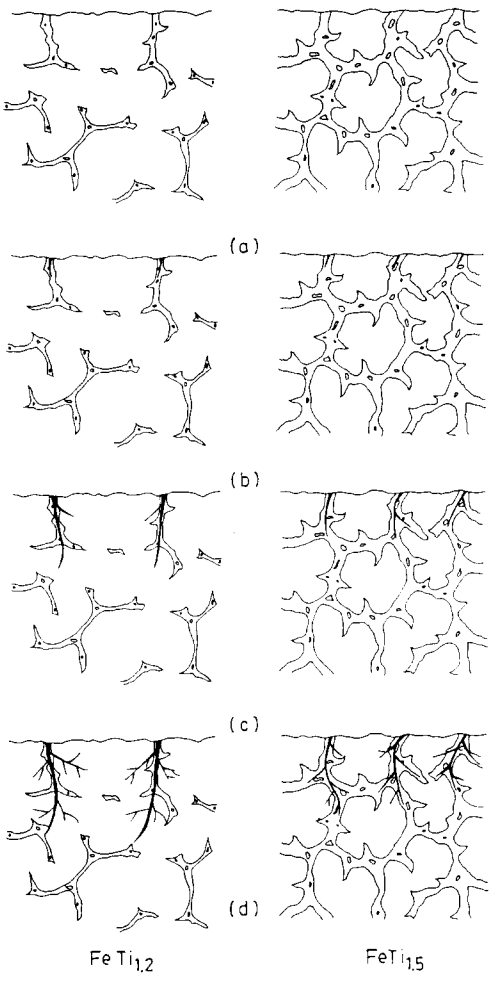

Fig. 8. Schematic comparison of hydrogen absorption and cracking process in the early stage for $FeTi_{1.2}$ and $FeTi_{1.5}$: (a) Cross sections of the alloys before hydrogenation; (b) Hydrogen is preferentially absorbed by β-Ti, causing some small cracks in the eutectic; (c) Cracking into the FeTi matrix has occurred in $FeTi_{1.2}$ and more hydrogen is absorbed, but the cracks in $FeTi_{1.5}$ remain in the eutectic; (d) More cracks are generated in the FeTi matrix of $FeTi_{1.2}$. In $FeTi_{1.5}$, some smaller cracks are also induced in the matrix.

first cycle, these micrographs can be used to compare the crack size after the first hydrogenation is completed. It is seen that the size of primary cracks indeed decreases as x increases.

In these micrographs, it is also observed that some small white flakes are present on the surface, most of them being near the primary cracks. EDX analysis shows that they contain slightly more titanium than the bulk. It is suspected that they are the FeTi particles originally present within the eutectic strips. During hydrogenation, some of them emerged from inside the primary cracks and were left on the surface after the original particles

had been pulverized into smaller granules. It is also noted that after hydrogenation, $FeTi_{1.5}$ remained fairly tough, whereas $FeTi_{1.2}$ could be further pulverized to even smaller granules quite easily. Again this is owing to the increased presence of β-Ti in $FeTi_{1.5}$.

5. Summary

Six alloys of $FeTi_{1+x}$ ($x=0$ to 0.5) were prepared and the hydrogen absorption–desorption properties were investigated. The alloys with excess titanium consisted of the FeTi matrix and eutectics of β-Ti and FeTi. When they were exposed to hydrogen, titanium hydride formed first. The large volume expansion of β-Ti during hydrogenation created large primary cracks along the eutectic strips and also induced many smaller cracks in FeTi. The clean surfaces generated in FeTi enabled the $FeTi_{1+x}$ alloys to absorb hydrogen without the activation treatment. The kinetics of the first hydrogenation cycle of these alloys was controlled by the number and distribution of the eutectic strips.

Acknowledgment

This work was supported by the National Science Council of Republic of China under Contract NSC 78-0405-E007-18.

References

1 *Metals Handbook*, Vol. 8, 8th edn., American Society of Metals, Metals Park, OH, 1973, p. 307.
2 J. J. Reilly and R. H. Wiswall, Jr., *Inorg. Chem.*, *13* (1974) 218.
3 T. Schober, *J. Less-Common Met.*, *89* (1983) 63.
4 C. S. Pande, M. A. Pick and R. L. Sabatini, *Scripta Metall.*, *14* (1980) 899.
5 J. J. Reilly and F. Reidinger, *J. Less-Common Met.*, *85* (1982) 145.
6 L. Schlapbach, A. Seiler, F. Stucki and H. C. Siegmann, *J. Less-Common Met.*, *73* (1980) 145.
7 T. Matsumoto and M. Amano, *Scripta Metall.*, *15* (1981) 879.
8 T. Schober and D. G. Westlake, *Scripta Metall.*, *15* (1981) 913.
9 P. S. Rudman, *J. Less-Common Met.*, *89* (1983) 93.
10 H. C. Kim and Jai-Young Lee, *J. Less-Common Met.*, *105* (1985) 247.
11 C. N. Park and Jai-Young Lee, *J. Less-Common Met.*, *91* (1983) 189.
12 Jai-Young Lee, C. N. Park and S. M. Pyun, *J. Less-Common Met.*, *89* (1983) 163.
13 H. S. Chung, Jai-Young Lee and J. K. Park, *J. Less-Common Met.*, *108* (1985) 35.
14 G. D. Sandrock and P. D. Goodell, *J. Less-Common Met.*, *73* (1980) 161.
15 G. D. Sandrock, in A. F. Andresen and A. J. Maeland (eds.), *Hydrides for Energy Storage*, Pergamon, Oxford, 1978, p. 353.
16 T. Mizuno and T. Morozumi, *J. Less-Common Met.*, *84* (1982) 237.
17 T. Matsumoto, M. Amano and Y. Sasaki, *J. Less-Common Met.*, *88* (1982) 443.
18 J. J. Reilly and R. H. Wiswall, Jr., *Inorg. Chem.*, *6* (1967) 2220.